AD-A065 130 OHIO STATE UNIV COLUMBUS ELECTROSCIENCE LAB F/G 9/5
ELECTRICALLY SMALL ANTENNA STUDIES.(U)
JAN 79 E H NEWMAN, C H WALTER DAAG29-76-G-0067
UNCLASSIFIED ESL-4311-9 ARO-13331.5-EL NL

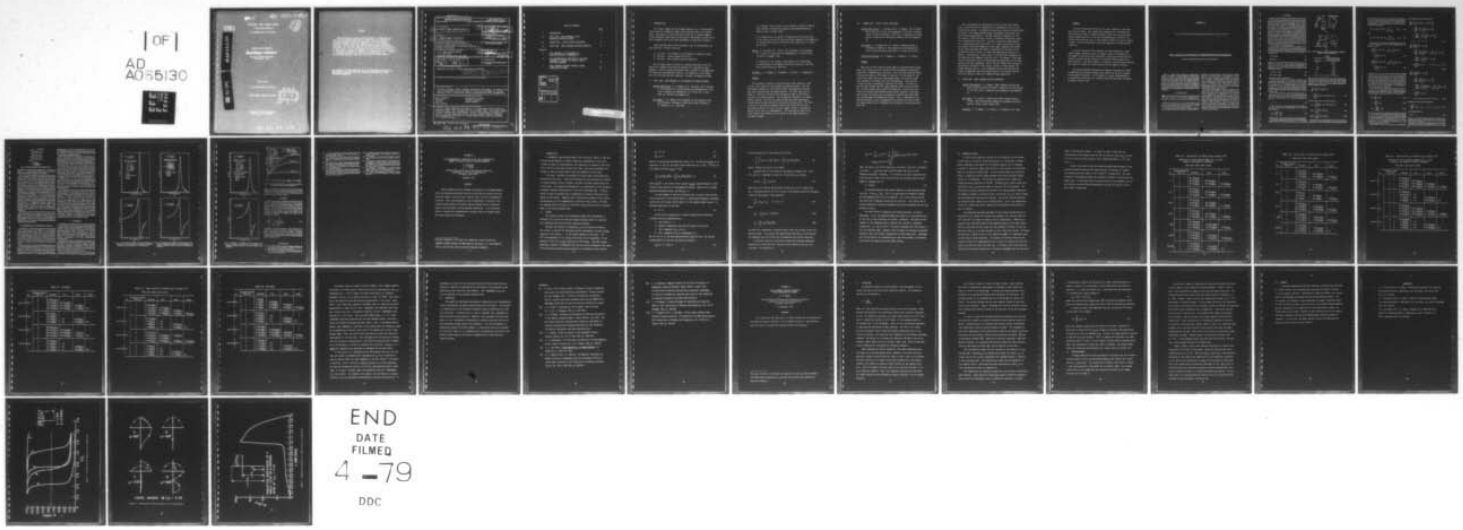

END
DATE FILMED
4 -79
DDC

[redacted] II

ARO 15331.5-EL

OSU

ELECTRICALLY SMALL ANTENNA STUDIES

Final Report 784311-9

E. H. Newman and C. H. Walter

12

NW

The Ohio State University

ElectroScience Laboratory

Department of Electrical Engineering
Columbus, Ohio 43212

January 1979

U. S. Army Research Office

Grant Number DAAG29-76-G-0057

NOTICES

When Government drawings, specifications, or other data are used for any purpose other than in connection with a definitely related Government procurement operation, the United States Government thereby incurs no responsibility nor any obligation whatsoever, and the fact that the Government may have formulated, furnished, or in any way supplied the said drawings, specifications, or other data, is not to be regarded by implication or otherwise as in any manner licensing the holder or any other person or corporation, or conveying any rights or permission to manufacture, use, or sell any patented invention that may in any way be related thereto.

THE FINDINGS IN THIS REPORT ARE NOT TO BE CONSTRUED AS AN OFFICIAL DEPARTMENT OF THE ARMY POSITION, UNLESS SO DESIGNATED BY OTHER AUTHORIZED DOCUMENTS.

UNCLASSIFIED

SECURITY CLASSIFICATION OF THIS PAGE (When Data Entered)

REPORT DOCUMENTATION PAGE

READ INSTRUCTIONS BEFORE COMPLETING FORM

1. REPORT NUMBER

2. GOVT ACCESSION NO.

3. RECIPIENT'S CATALOG NUMBER

4. TITLE (and Subtitle)

(6) ELECTRICALLY SMALL ANTENNA STUDIES.

(9) 5. TYPE OF REPORT & PERIOD COVERED

Final Report
15 Oct 75 - 14 Oct 78

6. PERFORMING ORG. REPORT NUMBER

ESL4311-9 (784311)

7. AUTHOR(s)

(10) E. H. Newman and C. H. Walter

8. CONTRACT OR GRANT NUMBER(s)

(15) Grant No. DAAG29-76-G-0067

9. PERFORMING ORGANIZATION NAME AND ADDRESS

The Ohio State University ElectroScience Laboratory, Department of Electrical Engineering
Columbus, Ohio 43212

10. PROGRAM ELEMENT, PROJECT, TASK AREA & WORK UNIT NUMBERS

11. CONTROLLING OFFICE NAME AND ADDRESS

(11)
U. S. Army Research Office
P. O. Box 12211
Research Triangle Park, NC 27709

12. REPORT DATE

Jan 1979

13. NUMBER OF PAGES

39 (12) 43p.

14. MONITORING AGENCY NAME & ADDRESS (if different from Controlling Office)

(14) ESL-4311-9
ESL-784311

15. SECURITY CLASS. (of this report)

Unclassified

15a. DECLASSIFICATION/DOWNGRADING SCHEDULE

16. DISTRIBUTION STATEMENT (of this Report)

Approved for public release; distribution unlimited.

(18) ARO (19) 13331.5-EL

17. DISTRIBUTION STATEMENT (of the abstract entered in Block 20, if different from Report)

18. SUPPLEMENTARY NOTES

The view, opinions, and/or findings contained in this report are those of the authors and should not be construed as an official Department of the Army position, policy, or decision, unless so designated by other documentation.

19. KEY WORDS (Continue on reverse side if necessary and identify by block number)

Small antennas
Dielectric
Ferrite
Wire antennas
Characteristic modes
Location synthesis
Moment methods

20. ABSTRACT (Continue on reverse side if necessary and identify by block number)

This report summarizes the work on U. S. Army Research Office Grant No. DAAG29-76-C-0067 from 15 October 1975 to 14 October 1978. Three areas related to small antennas were investigated: wires in the presence of dielectrical ferrites, closely spaced thin wires, and small antenna location synthesis. Each of these areas resulted in a journal publication, which are included in the Appendixes.

DD FORM 1 JAN 73 1473 EDITION OF 1 NOV 65 IS OBSOLETE

UNCLASSIFIED

SECURITY CLASSIFICATION OF THIS PAGE (When Data Entered)

JIB

TABLE OF CONTENTS

I. INTRODUCTION

This report summarizes the accomplishments on U. S. Army Research Office Grant No. DAAG29-76-C-0067 from 15 October 1975 to 14 October 1978. The purpose of this three year effort was to develop computational techniques applicable to the analysis and design of electrically small antennas, and to use these techniques to study small antennas.

Three separate topics were considered, each of approximately one year duration. Briefly, they are:

1) 1st year - wire antennas in the presence of material bodies
2) 2nd year - closely spaced thin wires
3) 3rd year - small antenna location synthesis.

Each of these topics resulted in a journal publication and this report will summarize the work and indicate its relevance to small antennas. The full journal publications are included in the Appendixes for those desiring additional details. The summaries in this report also list oral publications, personnel involved, and degrees granted.

II. FIRST YEAR - WIRE ANTENNAS IN THE PRESENCE OF MATERIAL BODIES

Journal Publication E. H. Newman and P. Tulyathan, "Wire Antennas in the Presence of a Dielectric/Ferrite Inhomogeneity," IEEE Trans. Antennas and Propagation, Vol. AP-26, No. 4, July 1978, pp. 587-593 (see Appendix A).

Oral Papers E. H. Newman, "Wire Antennas in the Presence of Material Bodies," Workshop on Electrically Small Antennas," Ft. Monmouth, N. J., May 1976.

E. H. Mewman, "Wire Antennas in the Presence of Material Bodies," 1976 IEEE/APS International Symposium and USNC/URSI Meeting, Amherst, Mass., October 19746.

E. H. Newman and C. H. Walter, "A Comparison of the Efficiency of the Electrically Small Dipole and Loop Antennas," 1977 Symposium on Antenna Applications at Allerton House, Monticello, Illinois, April 1977.

Degrees P. Tulyathan, M.S. Thesis, "Wire Antennas in the Presence of a Dielectric and/or Ferrite Inhomogeneity," The Ohio State University, December 1976.

P. Mangiacotti, M.S. Thesis, "The Effects of the Human Body on the Patterns of the Manpack Transceiver Antennas," The Ohio Ohio State University, June 1977.

Personnel E. H. Newman, P. Tulyathan, C. H. Walter, P. Mangiacotti.

Summary

Wire antennas in general, and electrically small antennas in particular, often operate in the presence of material bodies. The two most common examples are the ferrite loaded loop antenna and the manpack whip radiating near the human operator. In these cases the antenna is a thin-wire structure and the material body is the ferrite loading or the human operator. This problem was analyzed via a moment method solution. The wire and material body were both represented by equivalent currents which were evaluated in the solution. The technique and its associated computer code are applicable to thin wire and material bodies of fairly arbitrary shape. Further, the material bodies can be lossy and inhomogeneous. The technique was used to analyze loaded loop antennas and the effects of the human operator on a manpack antenna.

III. SECOND YEAR - CLOSELY SPACED THIN-WIRES

Journal Publication P. Tulyathan and E. H. Newman, "The Circumferential Variation of the Axial Component of Current in Closely Spaced Thin-Wire Antennas," IEEE Trans. on Antennas and Propagation, scheduled for publication January 1979 (see Appendix B).

Oral Paper E. H. Newman and C. H. Walter, "Recent Advances in the Method of Moments," 1977 Symposium on Antenna Applications at Allerton House, Monticello, Illinois, April 1977.

Scientific Personnel E. H. Newman, P. Tulyathan, C. H. Walter.

Summary

When two (or more) parallel wires come in close proximity to each other, this causes the axial current to be non-uniformly distributed around the circumference of the wires. This so-called proximity effect increases the ohmic or I^2R losses of the wire. In the design of the electrically small multiturn loop antenna (MTL), the turns are kept close together to minimize the size of the antenna. Also the wire is kept as thick as possible to minimize I^2R losses. Initially as the wire gets thicker the I^2R losses decrease since the wire current has a larger surface area on which to spread out. As wire size continues to increase the proximity effect losses increase to the point that further increasing wire size actually increases the total ohmic loss and decreases the antenna efficiency. Thus, a knowledge of the proximity effects or the circumferential distribtion of axial current in closely spaced wires is important to the design of the electrically small MTL.

The circumferential distribution of axial current was studied using a Fourier Series to represent the circumferential (or ϕ) variation of the current. In addition to providing a design tool applicable to the MTL, this study provided useful information and insight into the thin-wire approximation. The most important assumption in thin-wire theory is that the axial current is uniformly distributed around the circumference of the wire. In order to make this approximation it is required that the wire radius $a << \lambda$ and no two parallel wires pass within a few wire diameters of each other. However, the results of our study indicated that there is substantial ϕ variation of the current for wire of radius $a = 0.001\lambda$ and separated by 100 wire diameters. The question is then raised if the thin-wire assumption and the many thin-wire computer codes are valid. The answer is that they are valid and useful tools for predicting such quantities as far zone patterns and input impedance. While thin-wire theory does not predict the proper ϕ variation of the surface current, it does predict the proper average (over ϕ). Since impedance and far-zone patterns are primarily dependent upon the average values of the surface current, thin-wire theory is useful for computing these quantities.

IV. THIRD YEAR - SMALL ANTENNA LOCATION SYNTHESIS

Journal Publication E. H. Newman, "Small Antenna Location Synthesis Using Characteristic Modes," submitted for publication to the IEEE Trans. on Antennas and Propagation (see Appendix C).

Oral Paper C. H. Walter, "Electrically Small Antenna Studies at OSU," 1978 International Symposium on Antennas and Propagation, Sendai, Japan, August 1978.

Personnel E. H. Newman, C. H. Walter, P. Tylyathan, D. W. Epps

Summary

The usual problem with electrically small antennas is that they have low efficiency. The conventional approaches to increasing the efficiency are either to reduce the ohmic losses (say, by using thick highly conducting wires or low loss tuning/matching circuits) or to increase the radiation (say, by top loading a dipole or ferrite loading a loop). Here we investigate a different approach to increasing the radiation.

In actual operation small antennas are often mounted on a much larger support structure, such as a jeep, a ship, an airplane, etc. The support structure can be an effective radiator providing that substantial currents can be excited on it and that these currents are good radiators. The small antenna is viewed not as the primary radiator, but rather as a probe to excite currents on the support structure.

The design procedure developed here employs characteristic modes to determine the optimum frequency and location of the small antenna on the support structure. In an example of a small loop mounted on a crossed wire structure, the radiation and efficiency were increased by about a factor of 65.

APPENDIX A

IEEE TRANSACTIONS ON ANTENNAS AND PROPAGATION, VOL. AP-26, NO. 4, JULY 1978

Wire Antennas in the Presence of a Dielectric/Ferrite Inhomogeneity

EDWARD H. NEWMAN, MEMBER, IEEE, AND P. TULYATHAN

Abstract—A moment method solution for treating thin-wire antennas in the presence of an arbitrary dielectric and/or ferrite inhomogeneity is presented. The wire is modeled by an equivalent surface current density, and the dielectric/ferrite inhomogeneity is modeled by equivalent volume polarization currents. The conduction currents on the wire and the polarization currents in the dielectric/ferrite inhomogeneity are treated as independent unknowns and determined in the moment method solution. The method is applied to the problem of a loop antenna loaded with dielectric or ferrite. Numerical results are presented, and are in good agreement with measurements and previous calculations.

I. INTRODUCTION

THE INTERACTION of electromagnetic fields with metallic as well as dielectric and/or ferrite inhomogeneities is a problem of practical interest. Numerous techniques have been employed by various authors to treat antenna or scattering problems with dielectric/ferrite inhomogeneities [1]–[5]. Each of the above analyses treated a specific or very limited class of antennas or inhomogeneities. Often the geometries were two-dimensional or coincided with a separable coordinate system. It is desirable to have a single method to analyze a general class of problems where the antennas, scatterers, and inhomogeneities can be of arbitrary shape, and the inhomogeneities can be dielectric and/or ferrite.

The purpose of this paper is to present a moment method solution [6] to the problem of thin-wire antennas and scatterers in the presence of a dielectric/ferrite body. The analysis has the advantage that it is applicable to a wide variety of antenna, scatterer, and dielectric/ferrite geometries. It is sufficiently general to treat isotropic, lossy, and inhomogeneous bodies. The dielectric/ferrite inhomogeneities are modeled by equivalent volume polarization currents, and the wire is modeled by equivalent surface currents. The complex magnitudes of these currents are determined in the course of the moment method solution. The electrical sizes of the antennas, scatterers, and dielectric/ferrite inhomogeneities are limited by the finite computer storage.

Manuscript received February 13, 1977; revised September 14, 1977. This work was supported in part between the U.S. Army Research Office, Research Triangle Park, NC, and the Ohio State University Research Foundation under Grant DAAG29-76-G-0067.

The authors are with the ElectroScience Laboratory, Department of Electrical Engineering, Ohio State University, Columbus, OH 43212.

II. THEORY

Following the development of Richmond [7] and Newman [8], the moment method solution for thin-wire antennas and scatterers in the presence of a linear isotropic dielectric and/or ferrite inhomogeneity will now be developed. Fig. 1(a) shows the geometry to be considered. The impressed sources $(\mathbf{J}_i, \mathbf{M}_i)$ are confined to the volume V_1, and radiate the field (E, H) in the presence of two inhomogeneities. The first inhomogeneity is a thin-wire structure in the volume V_w and enclosed by the surface S_w. The second inhomogeneity is the dielectric/ferrite body in the volume V_2. The permittivity and permeability of this inhomogeneity are defined by the parameters (μ, ϵ), which may be complex functions of position. Although for simplicity not shown here, μ and ϵ could be considered as tensor quantities. This would permit the treatment of anisotropic inhomogeneities. The ambient medium has parameters (μ_0, ϵ_0). All sources and fields are considered to be time harmonic, and the $e^{j\omega t}$ time dependence will be suppressed.

The first step in the solution will be to replace the two inhomogeneities by equivalent sources. Employing the surface equivalence principle of Schelkunoff [9], the wire is removed and the following surface current densities are introduced on the surface S_w:

$$\mathbf{J}_s = \hat{n} \times \mathbf{H} \tag{1}$$

$$\mathbf{M}_s = \mathbf{E} \times \hat{n} \tag{2}$$

where $\hat{n}$ is the outward directed normal vector on S_w. By defining $(\mathbf{J}_s, \mathbf{M}_s)$ as in (1) and (2), the total field inside the wire is zero. Next, the dielectric/ferrite inhomogeneity is replaced by the ambient medium and the equivalent volume polarization currents

$$\mathbf{J} = j\omega(\epsilon - \epsilon_0)\mathbf{E} \tag{3}$$

$$\mathbf{M} = j\omega(\mu - \mu_0)\mathbf{H} \tag{4}$$

which are confined to the volume V_2.

The equivalent problem is shown in Fig. 1(b). Here, in the homogeneous medium (μ_0, ϵ_0), the sources $(\mathbf{J}_i, \mathbf{M}_i)$, $(\mathbf{J}_s, \mathbf{M}_s)$, and (J, M) radiate the field (E, H) exterior to S_w and the field (0, 0) interior to S_w. We use the notation that the sources $(\mathbf{J}_i, \mathbf{M}_i)$, $(\mathbf{J}_s, \mathbf{M}_s)$, (J), and (M), radiating in the ambient medium (μ_0, ϵ_0), produce the fields $(\mathbf{E}_i, \mathbf{H}_i)$, $(\mathbf{E}_s, \mathbf{H}_s)$, $(\mathbf{E}^J, \mathbf{H}^J)$, and $(\mathbf{E}^H, \mathbf{H}^H)$, respectively. These relationships are summarized in Table I.

Let us consider the wire to have a circular cross section. At each point on the wire we define a local right-handed orthogonal coordinate system with unit vectors $(\hat{n}, \hat{\phi}, \hat{l})$ where $\hat{n}$ is the outward normal vector to S_w, $\hat{l}$ is directed along the wire axis, and

$$\hat{\phi} = \hat{l} \times \hat{n}. \tag{5}$$

If the wire radius $a \ll \lambda$, then the surface current density on the wire structure can be approximated by the "thin-wire approximation"

$$\mathbf{J}_s(l) = \frac{\hat{l} I(l)}{2\pi a} = \frac{\mathbf{I}(l)}{2\pi a} \tag{6}$$

where $I(l)$ is the total current (conduction plus displacement).

The reaction integral equation (RIE) for $I(l)$ is obtained by placing a test source with current $(\mathbf{J}_m, \mathbf{M}_m)$ in V_w, and noting

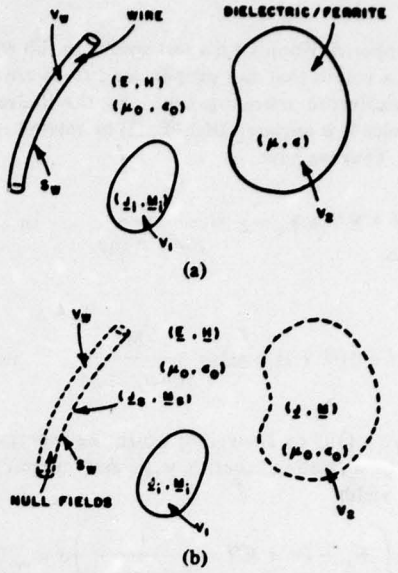

Fig. 1. (a) Wire antenna in presence of dielectric and/or ferrite inhomogeneity. (b) Equivalent problem.

TABLE I

Source Current	Field of the source radiating in the ambient medium (μ_0, ϵ_0)
$(\mathbf{J}_s, \mathbf{M}_s)$	$(\mathbf{E}_s, \mathbf{H}_s)$
$\mathbf{J}$	$(\mathbf{E}^J, \mathbf{H}^J)$
$\mathbf{M}$	$(\mathbf{E}^M, \mathbf{H}^M)$
$(\mathbf{J}_i, \mathbf{M}_i)$	$(\mathbf{E}_i, \mathbf{H}_i)$
$(\mathbf{J}_m, \mathbf{M}_m)$	$(\mathbf{E}^m, \mathbf{H}^m)$
$\mathbf{I}_n$	$(\mathbf{E}_{sn}, \mathbf{H}_{sn})$
$\mathbf{C}_n$	$(\mathbf{E}^J_n, \mathbf{H}^J_n)$
$\mathbf{Q}_n$	$(\mathbf{E}^M_n, \mathbf{H}^M_n)$

that since a null field exists in V_w, $(\mathbf{J}_m, \mathbf{M}_m)$ will have zero reaction with the sources $(\mathbf{J}_i, \mathbf{M}_i)$, $(\mathbf{J}_s, \mathbf{M}_s)$, and (J, M). Denoting $(\mathbf{E}^m, \mathbf{H}^m)$ as the fields radiated by $(\mathbf{J}_m, \mathbf{M}_m)$ in the ambient medium (μ_0, ϵ_0) and Z_s as the wire surface impedance for exterior excitation, the RIE is

$$-\int_0^L I(l)(E_l^m - Z_s H_\phi^m)\, dl$$

$$-\iiint_{V_2} (\mathbf{J} \cdot \mathbf{E}^m - \mathbf{M} \cdot \mathbf{H}^m)\, dv = V_m \tag{7}$$

where L represents the overall wire length and

$$V_m = \iiint_{V_1} [(\mathbf{J}_i \cdot \mathbf{E}^m - \mathbf{M}_i \cdot \mathbf{H}^m)\, dv \tag{8}$$

$$E_l^m = \frac{1}{2\pi}\int_0^{2\pi} (\hat{l} \cdot \mathbf{E}^m)\, d\phi \tag{9}$$

$$H_\phi^m = \frac{1}{2\pi}\int_0^{2\pi} (\hat{\phi} \cdot \mathbf{H}^m)\, d\phi. \tag{10}$$

Equation (7) is an integral equation for the three unknown currents $I(l)$, J, and M. This equation insures that these currents

have the proper reaction with a test source in the wire surface, but does not insure that the proper conditions are satisfied in the dielectric/ferrite inhomogeneity. In the dielectric/ferrite inhomogeneity it is required that (**E**, **H**) be related to (**J**, **M**) by (3) and (4). Thus we have

$$\mathbf{E}_s + \mathbf{E}^J + \mathbf{E}^H + \mathbf{E}_i = \mathbf{E} = \frac{\mathbf{J}}{j\omega(\epsilon - \epsilon_0)}, \qquad \text{in } V_2 \tag{11}$$

and

$$\mathbf{H}_s + \mathbf{H}^J + \mathbf{H}^H + \mathbf{H}_i = \mathbf{H} = \frac{\mathbf{M}}{j\omega(\mu - \mu_0)}, \qquad \text{in } V_2. \tag{12}$$

Multiplying (11) by the vector weighting function $\mathbf{w}_m$, (12) by the vector weighting function $\mathbf{w}_m'$, and integrating over the volume V_2 yields

$$\iiint_{V_2} \left(\mathbf{E}_s + \mathbf{E}^J + \mathbf{E}^H - \frac{\mathbf{J}}{j\omega(\epsilon - \epsilon_0)} \right) \cdot \mathbf{w}_m \, dv = -\iiint_{V_2} \mathbf{E}_i \cdot \mathbf{w}_m \, dv \tag{13}$$

$$\iiint_{V_2} \left(\mathbf{H}_s + \mathbf{H}^J + \mathbf{H}^H - \frac{\mathbf{M}}{j\omega(\mu - \mu_0)} \right) \cdot \mathbf{w}_m' \, dv = -\iiint_{V_2} \mathbf{H}_i \cdot \mathbf{w}_m' \, dv. \tag{14}$$

Equations (7), (13), and (14) are three coupled integral equations which can be solved for the unknown currents $I(l)$ and (**J**, **M**). The moment method solution to these equations is presented below. Strictly speaking, (7), (13), and (14) must be satisfied by an arbitrary ($\mathbf{J}_m$, $\mathbf{M}_m$), $\mathbf{w}_m$, and $\mathbf{w}_m'$. However, in the moment method solution we only enforce these equations for N distinct ($\mathbf{J}_m$, $\mathbf{M}_m$), M distinct $\mathbf{w}_m$, and P distinct $\mathbf{w}_m'$. In this case (7), (13), and (14) represent N, M, and P simultaneous linear integral equations, respectively.

The next step in the moment method solution will be to transform these simultaneous linear integral equations to simultaneous linear algebraic equations. This is accomplished by expanding the unknown currents **I**, **J**, and **M** as follows:

$$\mathbf{I}(l) = \sum_{n=1}^{N} I_n \mathbf{F}_n(l) \tag{15a}$$

$$\mathbf{J} = \sum_{n=N+1}^{N+M} I_n \mathbf{G}_n \tag{15b}$$

$$\mathbf{M} = \sum_{n=N+M+1}^{N+M+P} I_n \mathbf{Q}_n. \tag{15c}$$

In (15) the wire current is expanded in terms of the basis set $\mathbf{F}_n$, and the electric and magnetic volume polarization currents in terms of the basis sets $\mathbf{G}_n$ and $\mathbf{Q}_n$, respectively. To simplify the following equations we will denote ($\mathbf{E}_{sn}$, $\mathbf{H}_{sn}$), ($\mathbf{E}_n{}^J$, $\mathbf{H}_n{}^J$), and ($\mathbf{E}_n{}^H$, $\mathbf{H}_n{}^H$) as the fields radiated by $\mathbf{F}_n$, $\mathbf{G}_n$, and $\mathbf{Q}_n$, respectively, in the homogeneous medium (μ_0, ϵ_0). This notation is summarized in Table I.

Substituting (15) into (7), (13), and (14), and changing the order of integration and summation yields

$$\sum_{n=1}^{N} I_n \left\{ -\int_0^L F_n(l)(E_l{}^m - Z_s H_\phi{}^m) \, dl \right\} + \sum_{n=N+1}^{N+M} I_n \left\{ -\iiint_{V_2} \mathbf{G}_n \cdot \mathbf{E}^m \, dv \right\} + \sum_{n=N+M+1}^{N+M+P} I_n \left\{ +\iiint_{V_2} \mathbf{Q}_n \cdot \mathbf{H}^m \, dv \right\} = V_m, \qquad m = 1, 2, \cdots, N \tag{16a}$$

$$\sum_{n=1}^{N} I_n \left\{ \iiint_{V_2} \mathbf{E}_{sn} \cdot \mathbf{w}_m \, dv \right\} + \sum_{n=N+1}^{N+M} I_n \left\{ \iiint_{V_2} \left(\mathbf{E}_n{}^J - \frac{\mathbf{G}_n}{j\omega(\epsilon - \epsilon_0)} \right) \cdot \mathbf{w}_m \, dv \right\} + \sum_{n=N+M+1}^{N+M+P} I_n \left\{ \iiint_{V_2} \mathbf{E}_n{}^H \cdot \mathbf{w}_m \, dv \right\} = -\iiint_{V_2} \mathbf{E}_i \cdot \mathbf{w}_m \, dv, \qquad m = N+1, N+2, \cdots, N+M \tag{16b}$$

$$\sum_{n=1}^{N} I_n \left\{ \iiint_{V_2} \mathbf{H}_{sn} \cdot \mathbf{w}_n' \, dv \right\} + \sum_{n=N+1}^{N+M} I_n \left\{ \iiint_{V_2} \mathbf{H}_n{}^J \cdot \mathbf{w}_m' \, dv \right\} + \sum_{n=N+M+1}^{N+M+P} I_n \left\{ \iiint_{V_2} \left(\mathbf{H}_n{}^H - \frac{\mathbf{Q}_n}{j\omega(\mu - \mu_0)} \right) \cdot \mathbf{w}_m' \, dv \right\} = -\iiint_{V_2} \mathbf{H}_i \cdot \mathbf{w}_m' \, dv, \qquad m = N+M+1, N+M+2, \cdots N+M+P. \tag{16c}$$

Equation (16) can be written compactly as

$$\sum_{n=1}^{N+M+P} I_n Z_{mn} = V_m, \qquad m = 1, 2, \cdots, N+M+P \tag{17}$$

or in the matrix form as

$$ZI = V \tag{18}$$

where Z is the square impedance matrix, V is the excitation voltage column, and I is the current column which contains the unknown coefficients I_n, $n = 1, 2, \cdots, N+M+P$, as defined in (15). In Fig. 2, the impedance matrix Z is symbolically shown divided into nine regions, and the type of coupling

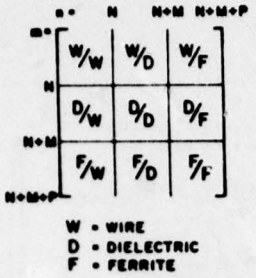

Fig. 2. Symbolic representation of impedance matrix Z.

accounted for in each region is indicated. In (16b) and (16c), when $m = n$, one must evaluate fields inside a current distribution. This problem is discussed in the Appendix.

In order to obtain numerical results from the above formulation, it is necessary to define specific expansion and weighting functions. The choices made for this study will now be presented. For $\mathbf{F}_n$ we choose the piecewise-sinusoidal function used by Richmond [7]. The unit magnitude vector volumetric pulse function is chosen for the expansion modes $\mathbf{G}_n$ and $\mathbf{Q}_n$. The volumetric pulses are the parallelepipeds obtained by dividing the dielectric/magnetic body into smaller rectangular volumes. Since the volume polarization current has an arbitrary polarization, it is necessary to have three orthogonal vector volumetric pulses occupying the same parallelepiped. Each will have a different polarization, i.e., $\hat{x}$, $\hat{y}$, and $\hat{z}$. There are no magnetic test sources and $\mathbf{M}_m = 0$. The piecewise-sinusoidal test function is chosen for $\mathbf{J}_m$. The choice of piecewise-sinusoidal functions for both the expansion and test modes enables us to use the computer program for thin-wire antennas and scatterers in a homogeneous medium, developed by Richmond [10], to calculate the wire/wire region of the impedance matrix Z. For the $\mathbf{w}_m$ or $\mathbf{w}_m'$ we choose a delta function which is located in the center of the corresponding volumetric pulse expansion $\mathbf{G}_m$ or $\mathbf{Q}_m$, and with the same polarization.

Since the test modes in the wire structure have the same current distribution as the expansion mode, this may be regarded as an application of Galerkin's method. The use of delta functions as the test modes for the dielectric/ferrite inhomogeneity results in (13) and (14) being satisfied at discrete points in V_2. This may be recognized as an application of the point-matching method.

III. EXPERIMENTAL AND NUMERICAL RESULTS

In this section, numerical results based on equations derived in the preceding section are presented for a loop antenna loaded with a dielectric and/or ferrite core. The calculated input admittance of the dielctric loaded loops are compared with experimental results. In the case of ferrite loaded loops, the computed radiation resistances are compared with the previous theoretical results by Stewart [1]. The loop geometry was chosen because it is a basic geometry and yet still required treating wire segments which are parallel or intersect at an angle.

The measurements were made with a half-loop mounted on a 4-ft square aluminum ground plane. The half-loop is made of copper wire coated with a thin layer of tin and has a total diameter of 0.032 in. The coaxial feed has an inner radius of 1/16 in and an outer radius of 3/8 in. The half-loop has a dimension of 3.02 in by 1.51 in. The dielectrics are rectangular parallelepipeds and have the dimensions $D1/2$, $D2$, and $D3$. The calculations were made for the complete loop, and it is the complete loop admittances which are plotted. The feed was modeled by a delta-gap generator.

Three examples will now be presented to demonstrate the ability of the theory to treat different types of dielectric inhomogeneities. Figs. 3(a) and (b) compare measured and calculated admittance of the loop loaded with Eccoflo-Hik ($\epsilon_r = 10.0$, produced by Emerson and Cuming). The dimensions of the block are $D1 = 2.60$ in, $D2 = 2.36$ in, and $D3 = 1.02$ in.

Next, the ability of the theory and computer program to treat problems with inhomogeneous dielectrics will be demonstrated. As seen in the insert in Fig. 4(a), the loop is loaded with an inhomogeneous dielectric of the same size as was considered above. The dielectric is half-filled with Teflon ($\epsilon_r = 2.1$) and half-filled with Eccoflo-Hik. Figs. 4(a) and (b) show the measured and calculated admittance of the loaded loop.

Distilled water ($\epsilon_r = 78.05 - j3.74$ at the resonance frequency of the loop) is used to demonstrate the ability to treat lossy dielectrics. Due to the large relative permittivity of water, the size of the inhomogeneity has been reduced to $D1 = 1.97$ in, $D2 = 1.54$ in, and $D3 = 0.75$ in. The measured and calculated admittance of the water loaded loop are shown in Figs. 5(a) and (b).

One of the most common uses of ferrites is to increase the radiation resistance of loop antennas. Fig. 6 shows the radiation resistance of a ferrite loaded loop versus μ_r. Curves are shown for various sizes of the ferrite cores. The loop has a perimeter $L = 47.24$ in, and the ferrite cores are of size $D1 = 9.45$ in, $D2 = 9.45$ in, and $D3 = 2.36$ in, 11.81 in, and 23.62 in. The computations are at 50 MHz where the loop circumference is about 0.20λ. The present results are compared with the previous approximate results of Stewart. These two results are seen to agree only qualitatively. It is felt that most of the quantitative differences are due to approximations given by Stewart for the demagnetization factor of a rectangular rod. More recently, Pettengill *et al.* [11] have presented different expressions for the demagnitization factor of a core with length to diameter ratio greater than two. The $D3 = 23.62$ case is compared to a computation using Pettengill's demagnitization factor, and the agreement is good.

IV. SUMMARY

The purpose of this study has been to develop a technique to analyze thin-wire antennas and scatterers in the presence of a dielectric and/or ferrite inhomogeneity. The method presented is a moment method solution and a modification of the piecewise-sinusoidal reaction formulation for thin-wire antennas and scatterers in a homogeneous medium. The technique is sufficiently general to be applicable to lossy and loaded thin-wire antennas and scatterers in the presence of isotropic, inhomogeneous, and lossy dielectric/ferrite inhomogeneities.

Numerical results have been presented and compared with measurements and previous calculations. These results show the ability of the theory and computer program to analyze antennas in the presence of dielectrict of varying sizes and permittivities, inhomogeneous dielectrics, lossy dielectrics, and ferrites. The method is, however, limited by the finite computer core to electrically small inhomogeneities.

Using the technique presented here for treating antennas and scatterers in the presence of a dielectric/ferrite inhomo-

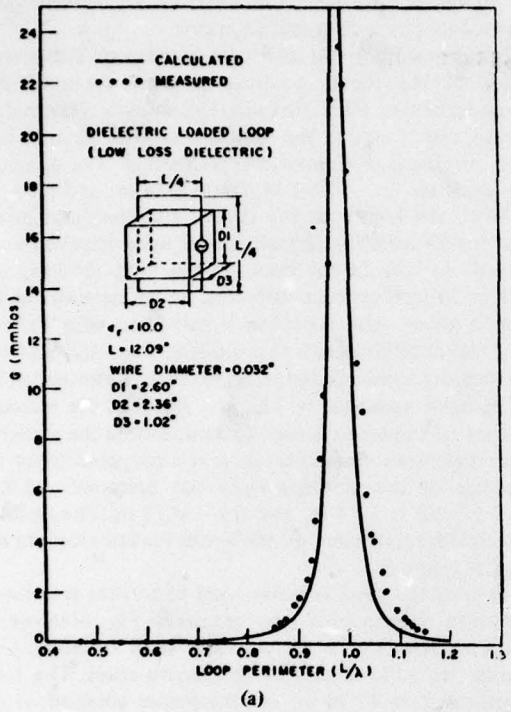

(a)

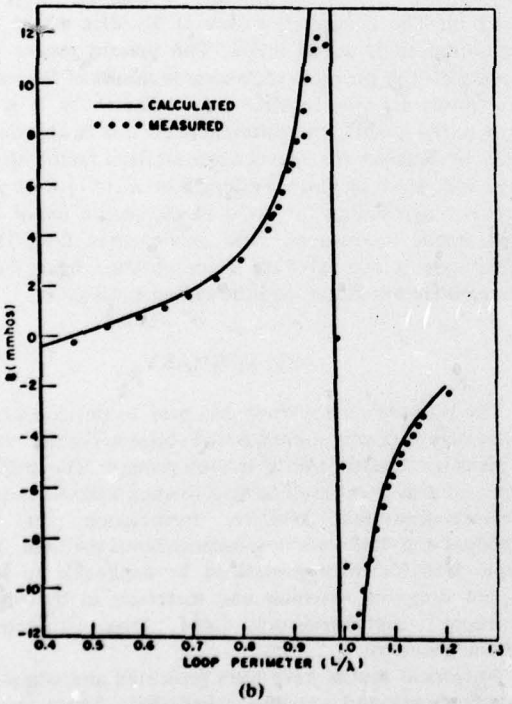

(b)

Fig. 3. (a) Comparison of calculated and measured conductance for dielectric (ϵ_r = 10.0) loaded loop. (b) Comparison of calculated and measured susceptance for dielectric (ϵ_r = 10.0) loaded loop.

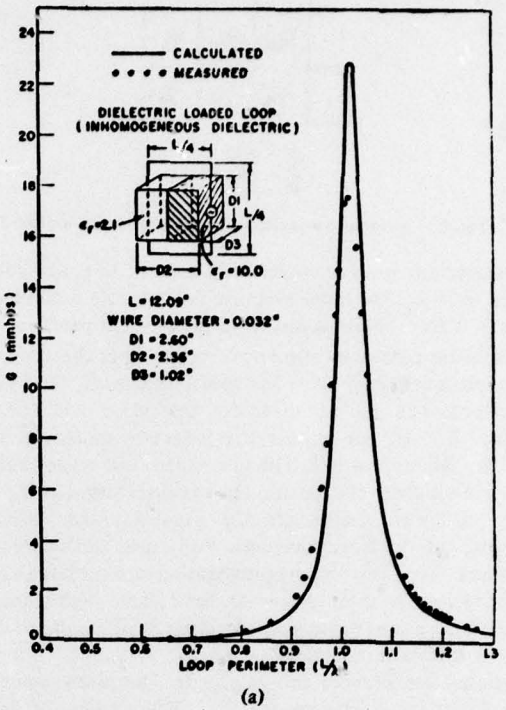

(a)

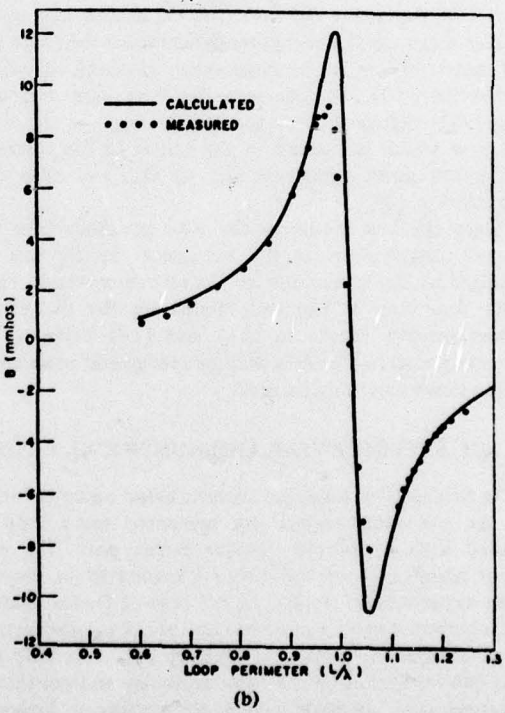

(b)

Fig. 4. (a) Comparison of calculated and measured conductance for dielectric (inhomogeneous) loaded loop. (b) Comparison of calculated and measured susceptance for dielectric (inhomogeneous) loaded loop.

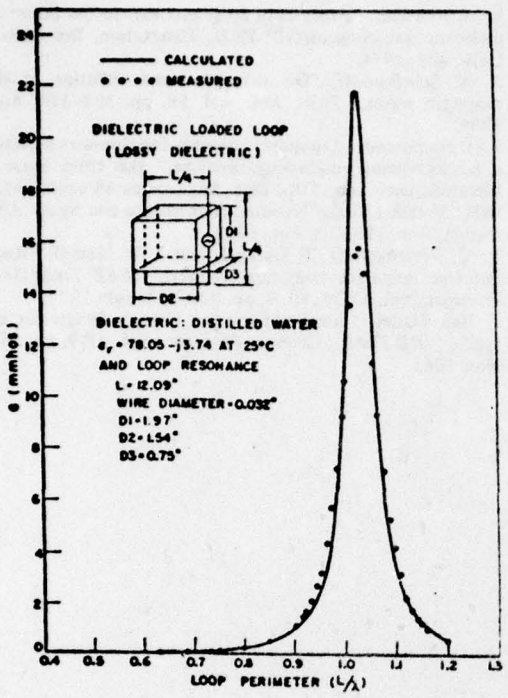

(a)

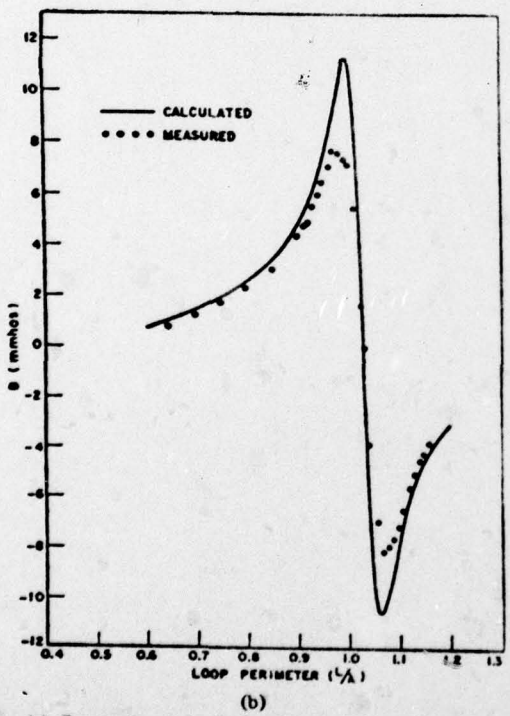

(b)

Fig. 5. (a) Comparison of calculated and measured conductance for dielectric (distilled water) loaded loop. (b) Comparison of calculated and measured susceptance for dielectric (distilled water) loaded loop.

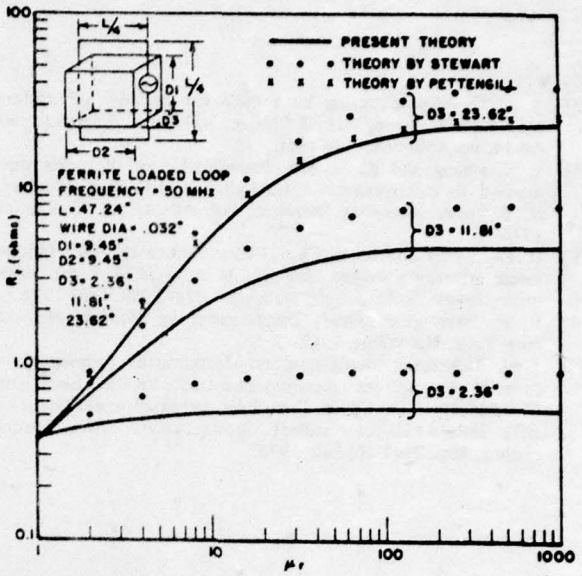

Fig. 6. Comparison of present theory with previous calculation for the radiation resistance of ferrite loaded loops.

geneity, one can analyze problems such as ferrite loaded loops, manpack transceiver antennas, scattering from rain or blood cells, effects of microwave radiation on biological tissues, and antennas covered by dielectric radomes.

APPENDIX

Consider the problem of finding the electric field at the center of a column of current with uniform current density $\mathbf{J} = \hat{z}J$, occupying a circular cylindrical volume. In numerically evaluating this field, one must exclude a small region about the field point. Unfortunately, the value of the resultant integral is dependent upon the shape of the volume excluded. If one excludes a circular cylinder of radius η and height $2h$ surrounding the singularity, Van Bladel [12] found that the result will be in error by

$$\delta = \left(1 - \frac{1}{\sqrt{1 + \frac{\eta^2}{h^2}}}\right) \frac{\mathbf{J}}{j\omega\epsilon_0}. \tag{A-1}$$

Note that if one excludes a long thin cylinder where $\eta \ll h$, δ goes to zero and the correct result is obtained. This idea is used in determining the electric field inside a volumetric electric current expansion mode, and also for the dual problem of determining the magnetic field inside a volumetric magnetic current expansion mode.

REFERENCES

[1] J. L. Stewart, "Research in magnetic antennas," California Inst. Tech.; prepared under Contract No. DA-36-039 sc-73189 for Signal Corps., Dep. of the Army, Sept. 13, 1957.

[2] J. H. Richmond, "Scattering by a dielectric cylinder of arbitrary cross section shape," *IEEE Trans. Antennas Propagat.*, vol. AP-13, pp. 334-341, May 1965.

[3] —, "TE-wave scattering by a dielectric cylinder of arbitrary cross-section shape," *IEEE Trans. Antennas Propagat.*, vol. AP-14, pp. 460–464, July 1966.

[4] S. K. Chang and K. K. Mei, "Application of the unimoment method to electromagnetic scattering of dielectric cylinders," *IEEE Trans. Antennas Propagat.*, vol. AP-24, pp. 35–42, Jan. 1976.

[5] D. E. Livesay and K. M. Chen, "Electromagnetic fields induced inside arbitrarily shaped biological bodies," *IEEE Trans. Microwave Theory Tech.*, vol. MTT-22, pp. 1273–1280, Dec. 1974.

[6] R. F. Harrington, *Field Computations by Moment Methods*. New York: MacMillan, 1968.

[7] J. H. Richmond, "Radiation and scattering by thin-wire structures in the complex frequency domain," the Ohio State Univ. ElectroScience Lab., Dep. Elec. Eng., prepared under Grant No. NGL 36-008-138 for National Aeronautics and Space Administration, Rep. 2902-10, July 1973.

[8] E. H. Newman, "Analysis of strip antennas in the presence of a dielectric inhomogeneity," Ph.D. dissertation, the Ohio State University, 1974.

[9] S. A. Schelkunoff, "On diffraction and radiation of electromagnetic waves," *Phys. Rev.*, vol. 56, pp. 308–316, Aug. 15, 1939.

[10] J. H. Richmond, "Computer program for thin-wire structures in a homogeneous conducting medium," the Ohio State Univ. ElectroScience Lab., Dep. Elec. Eng., prepared under Grant No. NGL 36-008-138 for National Aeronautics and Space Administration, Rep. 2902-12, Aug. 1973.

[11] R. C. Pettengill, H. T. Garland, and J. D. Meindl, "Receiving antenna design for miniature receivers," *IEEE Trans Antennas Propagat.*, vol. AP-25, no. 4, pp. 528–530, July 1977.

[12] J. Van Bladel, "Some remarks on Green's dyadic for infinite space," *IRE Trans. Antennas Propagat.*, vol. AP-9, pp. 563-566, Nov. 1961.

APPENDIX B

THE CIRCUMFERENTIAL VARIATION OF THE AXIAL COMPONENT OF CURRENT IN CLOSELY SPACED THIN-WIRE ANTENNAS*

P. Tulyathan
E. H. Newman

The Ohio State University ElectroScience Laboratory
Department of Electrical Engineering
Columbus, Ohio 43212

December 1977

ABSTRACT

Closely spaced thin-wire antennas are analyzed by the moment method using the piecewise-sinusoidal function to describe the current variation along the length of the wire and a Fourier series for the circumferential variation. Data are presented for the circumferential variation of the surface current density of parallel dipoles obtained by the "thin-wire" theory, wire-grid model, and the present formulation. It is found that there is substantial circumferential variation, even for dipoles spaced more than several wire diameters.

---

*The work reported in this paper was supported in part by Grant No. DAAG29-76-G-0067 between the Department of the Army, U. S. Army Research Office, and The Ohio State University Research Foundation.

I. INTRODUCTION

A fundamental approximation made in the "thin-wire" theory is that the surface current density is uniform around the circumference of the wires. In order to make this approximation, two conditions are imposed on the wires. First, the wire radius must be much less than a free space wavelength, and second, no two wires pass within a few wire diameters of each other.

This paper considers the problem of closely spaced three-dimensional electrically thin wires. Smith [1] and Olaofe [2] had considered the problem of closely spaced infinite cylinders, and Smith included a modification for finite wires. The solution presented here is a modification of the piecewise-sinusoidal reaction formulation for "thin wire" structures [3]. A Fourier series is used to represent the circumferential variation of the axial component of the current. Numerical data illustrate the effects of wire radius and separation on the circumferential variation of the current. The data are compared with the results of "thin-wire" theory and also with a wire-grid model of the closely spaced wires.

II. THEORY

The reaction concept was introduced by Rumsey [4], and applied by Richmond [3] to derive the reaction integral equation (RIE) for radiation and scattering from thin-wires and conducting surfaces.

Consider the problem of scattering by a wire structure enclosed by the surface S, and with the impressed electric and magnetic currents $(\underline{J}_i, \underline{M}_i)$ confined in the volume V. Let the ambient medium be free space. The $e^{j\omega t}$ time dependence of all sources and fields will be suppressed. In the presence of the wire, $(\underline{J}_i, \underline{M}_i)$ generate the field $(\underline{E}, \underline{H})$. From the surface-equivalence theorem of Schelkunoff [5], the wire can be replaced by free space if the following surface-current densities are introduced on the surface S

$$\underline{J}_s = \hat{n} \times \underline{H} \tag{1}$$

$$\underline{M}_s = \underline{E} \times \hat{n} \tag{2}$$

where $\hat{n}$ is the outward directed unit vector on S. By defining $(\underline{J}_s, \underline{M}_s)$ as in Equations (1) and (2), the total field inside the wire is zero. The RIE for the unknown currents $(\underline{J}_s, \underline{M}_s)$ is [3]

$$\iint_S (\underline{J}_s \cdot \underline{E}^m - \underline{M}_s \cdot \underline{H}^m) ds + \iiint_V (\underline{J}_i \cdot \underline{E}^m - \underline{M}_i \cdot \underline{H}^m) dv = 0 \tag{3}$$

where $(\underline{E}^m, \underline{H}^m)$ is the field of test sources $(\underline{J}_m, \underline{M}_m)$ located interior to the surface S and radiating in the homogeneous medium. Below we will consider perfectly-conducting wires, and thus $\underline{M}_s = 0$.

Let each segment of the wire structure have a circular cross section and at each point on the surface define a right-handed orthogonal coordinate system with unit vectors $(\hat{n}, \hat{\phi}, \hat{\ell})$ where $\hat{n}$ is the outward normal vector, $\hat{\ell}$ is directed along the wire axis and

$$\hat{\phi} = \hat{\ell} \times \hat{n}. \tag{4}$$

At this point, Equation (3) is usually simplified by making the following thin-wire approximations:

1. wire radius $a << \lambda$
2. neglect integrations over the end surfaces of the wire
3. the $\hat{\phi}$ component of $\underline{J}_s$ is zero
4. the $\hat{\ell}$ component of $\underline{J}_s$ is independent of ϕ.

We will use all of the above approximations except for #4. The surface current density on the wire can then be written as

$$\underline{J}_s(\ell, \phi) = \hat{\ell}\, J_s(\ell, \phi) \quad . \tag{5}$$

Inserting Equation (5) into Equation (3) yields

$$-\int_0^L \int_0^{2\pi} J_s(\ell,\phi)\ (\hat{\ell}\cdot\underline{E}^m)\ a\,d\phi\ d\ell = \iiint_V (\underline{J}_i\cdot\underline{E}^m - \underline{M}_i\cdot\underline{H}^m)dv \quad , \tag{6}$$

where L denotes the overall wire length.

Equation (6) will be solved via the method of moments [6]. To do this $J_s(\ell,\phi)$ is expanded in terms of a finite series as follows:

$$J_s(\ell,\phi) = \sum_{n=1}^{N} J_n\ G_n(\ell,\phi) \tag{7}$$

where the J_n are unknown coefficients and the $G_n(\ell,\phi)$ are a known basis set. Enforcing Equation (6) for N distinct test sources yields the following system of simultaneous linear equations

$$\sum_{n=1}^{N} J_n\ Z_{mn} = V_m \qquad m = 1,2,\cdots N \tag{8}$$

where

$$Z_{mn} = -\iint_n G_n(\ell,\phi)\ (\hat{\ell}\cdot\underline{E}^m)\ ds \tag{9a}$$

$$V_m = \iiint_V (\underline{J}_i\cdot\underline{E}^m - \underline{M}_i\cdot\underline{H}^m)dv \tag{9b}$$

and where the integration in Equation (9a) is over the surface of the n-th expansion mode. The accuracy and computational efficiency of the solution are dependent upon the choices for the expansion and testing functions.

In defining expansion functions we choose the piecewise-sinusoidal function [3] to describe the ℓ variation and a Fourier series for the ϕ variation. The expansion is

$$J_s(\ell,\phi) = \sum_{p=1}^{P} J_p F_p(\ell) + \sum_{k=1}^{K} \left\{ \sum_{p=1}^{P} \left[J_{(2k-1)P+p} F_p(\ell) \cos k\phi \right. \right.$$

$$\left. \left. + J_{2kP+p} F_p(\ell) \sin k\phi \right] \right\} . \qquad (10)$$

Thus, the $G_n(\ell,\phi)$ are of the form $F_n(\ell)$, $F_n(\ell)\cos\phi$, $F_n(\ell)\sin\phi$, $F_n(\ell)\cos 2\phi$, $F_n(\ell)\sin 2\phi$, $\cdots$ $F_n(\ell)\cos K\phi$ and $F_n(\ell)\sin K\phi$ where the $F_n(\ell)$ are the piecewise-sinusoidal V-dipoles. If P V-dipoles are used to describe the ℓ variation and K terms in the Fourier series are retained, then the total number of unknowns will be

$$N = P(2K+1). \qquad (11)$$

The testing functions were chosen identical to the expansion modes. Thus, $\underline{M}_m = 0$ and $\underline{J}_m = \hat{\ell} G_m$. This is an application of Galerkin's method and the impedance matrix will be symmetric. Our initial choice for the test modes was filamentary sources on the wire axis. This choice led to serious problems of relative convergence [7] and was abandoned for the true Galerkin solution.

The above choice of expansion and testing functions has several advantages. First, the expansion modes are placed in an overlapping array on the wire so that continuity of current is enforced. Evaluation of the elements in the impedance matrix, Equation (9), requires a quadruple integration, i.e., two to find $\underline{E}^m$ and two to integrate over the surface of the n-th expansion mode. However, since we employ the piecewise-sinusoidal functions, only two of these integrations are done numerically. Advantage can also be taken of the orthogonality of the Fourier modes in evaluating terms where the expansion and test modes overlap.

III. NUMERICAL RESULTS

In this section numerical results will be presented for the surface current density of parallel center-fed dipoles, as illustrated in Figure 1. Results obtained by the method of the previous section will be compared to those of "thin-wire" theory [8], and also to the results of a wire-grid model of the parallel dipoles [9]. In the wire-grid model each thin-wire dipole is modeled by about sixteen extremely thin wires uniformly spaced around its circumference. The dipoles are center-fed by in phase unit voltage delta-gap generators at 30 MHz. Although $\underline{J}_s(\ell,\phi)$ varies along the ℓ coordinate, only $\underline{J}_s$ around the center of the wire will be presented. The following calculations demonstrate the ability of the preceding formulation and computer programs to account for the ϕ variation of $\underline{J}_s$ for closely spaced thin and moderately thick parallel dipoles. The surface current densities are normalized with respect to an isolated dipole. In all the computations to follow, 3 modes were used to describe the longitudinal distribution on each $\lambda/2$ dipole.

The normalized magnitude and phase of the surface current density of two parallel $\lambda/2$ dipoles for various wire spacings, c/a, and wire radii of $10^{-3}\lambda$ and $10^{-2}\lambda$ are shown in Figures 2 and 3, respectively. Referring to Equation (10), the coefficients of the expansion modes for the above cases, and for a few cases of very large c/a, are presented in Tables 1-A and 1-B. Note that since $\underline{J}_s$ is an even function in ϕ all $\sin k\phi$ terms vanish. Following the notation of Equation (10), K will denote the number of ϕ dependent terms in the surface current expansion. For example, K=0 implies that only the constant ("thin-wire" approximation) term is used, K=1 implies that the constant, $\cos\phi$ and $\sin\phi$ terms are used, etc. In Figures 2 and 3 note that the results of the previous section are in excellent agreement with the wire-grid

model of the parallel dipoles. In Tables 1-A and 1-B note that the coefficients of the constant term for the K=0 case are very close to those of the K=1 and K=2 cases, except in the extreme case where $a = 10^{-2}\lambda$ and $c/a = 1.1$.

Figure 4 and Figure 5 show the normalized magnitude and phase of the surface current distribution for three parallel $\lambda/2$ dipoles for various wire spacings and wire radii of $10^{-3}\lambda$ and $10^{-2}\lambda$, respectively. The coefficients of the expansion modes are tabulated in Tables 2-A and 2-B for the above cases. In the cases where the wires are very close together (c/a=1.1 and c/a=2.0), the coefficients predicted by the case K=0 can be in error by an order of magnitude.

TABLE 1-A. Two Parallel $\lambda/2$ Dipoles Each of Radius $10^{-3}\lambda$

Coefficients of the Expansion Modes for J_s at the Center of the Dipole #1 (mA/meter)

Note that $\sin k\phi$ terms vanish

c/a	expansion mode used (K)	Constant	$\cos\phi$	$\cos 2\phi$
1.1	0	86.50/-26.6	-	-
	1	86.33/-26.5	166.29/149.4	-
	2	86.33/-26.5	164.65/149.4	34.12/152.0
2.0	0	86.06/-26.1	-	-
	1	86.00/-25.9	168.12/148.2	-
	2	86.00/-25.9	167.63/148.2	30.36/149.8
20.0	0	88.23/-20.2	-	-
	1	88.24/-20.1	166.23/143.8	-
	2	88.24/-20.1	166.23/143.8	4.11/150.6
50.0	0	97.59/-13.6	-	-
	1	97.64/-13.6	164.11/139.0	-
	2	97.64/-13.6	164.11/139.0	1.86/156.6
1,000	0	161.38/-31.8	-	-
	1	161.06/-31.8	46.23/-136.8	-
	2	161.06/-31.8	46.23/-136.8	0.26/-62.4
10,000	0	172.97/-27.7	-	-
	1	172.64/-27.7	5.02/-127.2	-
	2	172.64/-27.7	5.02/-127.2	0.03/-112.2
100,000	0	174.03/-27.7	-	-
	1	173.73/-27.2	0.51/-170.5	-
	2	173.73/-27.2	0.51/-170.5	0.0

TABLE 1-B. Two Parallel $\lambda/2$ Dipoles Each of Radius $10^{-2}\lambda$

Note that $\sin k\phi$ terms vanish

c/a	expansion mode used (K)	Constant	$\cos\phi$	$\cos 2\phi$
1.1	0	7.96/-15.7	-	-
	1	8.19/-13.7	20.64/149.0	-
	2	8.19/-13.6	20.49/148.8	5.10/157.4
2.0	0	8.03/-11.2	-	-
	1	8.32/-9.9	21.47/145.5	-
	2	8.32/-9.9	21.40/145.5	4.89/153.7
20.0	0	18.38/7.0	-	-
	1	18.35/6.7	24.51/83.1	-
	2	18.35/6.7	24.51/83.1	1.93/133.6
50.0	0	13.49/-26.9	-	-
	1	13.56/-26.4	10.90/-146.6	-
	2	13.56/-26.4	10.90/-146.6	0.82/-76.1
1,000	0	16.06/-20.3	-	-
	1	16.21/-19.7	0.66/-123.0	-
	2	16.21/-19.7	0.66/-123.0	0.05/-36.5
10,000	0	16.18/-19.8	-	-
	1	16.33/-19.2	0.07/-166.3	-
	2	16.33/-19.2	0.07/-166.3	0.0

TABLE 2-A. Three Parallel $\lambda/2$ Dipoles Each of Radius $10^{-3}\lambda$

Coefficients of the Expansion Modes for J_s at the Center of the Dipoles #1 and #2 (mA/meter)

Note that $\sin k\phi$ terms vanish

	c/a	expansion mode used (K)	Constant	$\cos\phi$	$\cos 2\phi$	$\cos 3\phi$
wire #1	1.1	0	139.36/-29.2	-	-	-
		1	79.47/-27.0	180.71/149.0	-	-
		2	83.79/-27.1	169.20/148.9	21.18/153.5	-
		3	84.25/-27.2	168.26/148.9	20.36/154.0	6.81/-38.4
wire #2	1.1	0	107.35/145.5	-	-	-
		1	13.26/-11.8	0.0	-	-
		2	5.73/17.0	0.0	66.09/151.4	-
		3	5.25/25.2	0.0	68.60/151.1	0.0
wire #1	2.0	0	101.48/-28.1	-	-	-
		1	85.41/-27.0	170.37/147.9	-	-
		2	85.78/-27.0	168.61/147.9	17.16/151.9	-
		3	85.78/-27.0	168.61/147.9	17.16/151.9	1.22/166.0
wire #2	2.0	0	33.54/136.0	-	-	-
		1	6.39/63.0	0.0	-	-
		2	6.53/70.5	0.0	60.49/149.2	-
		3	6.53/70.5	0.0	60.46/149.2	0.0

TABLE 2-A. Continued

	c/a	expansion mode used (K)	Constant	cosφ	cos2φ	cos3φ
wire #1	20.0	0	91.89/-21.2	-	-	-
		1	90.07/-20.9	170.14/143.7	-	-
		2	90.75/-20.9	170.14/143.7	2.51/160.0	-
		3	90.75/-20.9	170.14/143.7	2.51/160.0	0.0
wire #2	20.0	0	24.35/74.1	-	-	-
		1	23.69/68.7	-	-	-
		2	23.69/68.7	0.0	8.36/150.2	-
		3	23.69/68.7	0.0	8.36/150.2	0.0
wire #1	50.0	0	103.08/-13.9	-	-	-
		1	103.67/-13.7	169.30/138.4	-	-
		2	102.67/-13.7	169.30/138.4	1.51/173.1	-
		3	102.67/-13.7	169.30/138.4	1.51/173.1	0.0
wire #2	50.0	0	47.96/53.9	-	-	-
		1	47.96/52.7	0.0	-	-
		2	47.96/52.7	0.0	3.86/156.5	-
		3	47.96/53.7	0.0	3.86/156.5	0.0

TABLE 2-B. Three Parallel $\lambda/2$ Dipoles Each of Radius $10^{-2}\lambda$

Note that $\sin k\phi$ terms vanish

	c/a	expansion mode used (K)	Constant	$\cos\phi$	$\cos 2\phi$	$\cos 3\phi$
wire #1	1.1	0	14.67/-25.8	-	-	-
		1	7.27/-12.8	23.57/148.4	-	-
		2	7.82/-13.8	22.12/147.9	3.95/162.2	-
		3	7.89/-14.1	21.96/148.0	3.81/163.4	1.08/-51.7
wire #2	1.1	0	14.31/135.8	-	-	-
		1	2.40/17.6	0.0	-	-
		2	1.80/45.1	0.0	9.22/157.8	-
		3	1.82/50.2	0.0	9.62/156.6	0.0
wire #1	2.0	0	10.14/-17.9	-	-	-
		1	8.59/-11.9	21.96/145.3	3.42/163.0	-
		2	8.52/-11.8	22.28/145.3	-	-
		3	8.59/-11.9	21.96/145.3	3.42/163.0	0.34/-165.8
wire #2	2.0	0	5.97/113.1	-	-	-
		1	3.11/74.4	0.0	-	-
		2	3.16/76.7	0.0	10.10/152.7	-
		3	3.16/76.7	0.0	10.10/152.7	0.0

TABLE 2-B. Continued

	c/a	expansion mode used (K)	Constant	cosφ	cos2φ	cos3φ
wire #1	20.0	0	17.63/2.0	-	-	-
		1	17.76/2.5	20.69/78.2	-	-
		2	17.76/2.5	20.69/78.2	1.91/124.9	-
		3	17.76/2.5	20.69/78.2	1.91/124.9	0.07/159.4
wire #2	20.0	0	24.16/21.7	-	-	-
		1	23.83/22.1	0.0	-	-
		2	23.83/22.1	0.0	3.80/129.0	-
		3	23.83/22.1	0.0	3.80/129.0	0.0
wire #1	50.0	0	12.40/-28.9	-	-	-
		1	12.50/-28.4	14.54/-149.2	-	-
		2	12.50/-28.4	14.54/-149.2	1.09/-75.6	-
		3	12.50/-28.4	14.54/-149.2	1.09/-75.6	0.03/-8.6
wire #2	50.0	0	11.18/-34.8	-	-	-
		1	11.14/-34.6	0.0	-	-
		2	11.12/-34.6	0.0	1.55/-78.8	-
		3	11.12/-34.6	0.0	1.55/-78.8	0.0

The results shown in Figures 2-5 and in Tables 1 and 2 suggest opposite conclusions as to the accuracy of the usual thin-wire approximation that $\underline{J}_s$ is independent of ϕ. First, Figures 2-5 clearly show that $\underline{J}_s$ is strongly ϕ dependent, even for c/a as large as 50 and a as small as $\lambda/1000$. Thus, one is led to the conclusion that the thin-wire approximation is not valid. Next, Tables 1 and 2 show that, except for extremely small c/a where the thin-wire approximation is known to fail, the ϕ independent term predicted from "thin-wire" theory (K=0 case) is essentially identical to the ϕ independent term from the K=1 or K=2 cases. Since for wires whose radius $a \ll \lambda$ it is the ϕ independent term which dominates the far-zone radiated fields, "thin-wire" theory will predict the proper far-zone fields. Also, if the device used to measure input impedance is sensitive to the average value of voltage/J_s around the circumference of the wire, then it will also depend only on the ϕ independent modes. Thus, one can be led to the conclusion that the "thin-wire" approximation is in fact valid. This discrepency can be resolved by stating that the "thin-wire" approximation is not valid for predicting the circumferential distribution of current on a general wire structure. However, it is <u>useful</u> for computing such quantities as impedance and far-zone fields.

At this point it is reasonable to ask the question "why go to all the time and trouble to determine the ϕ dependence of $\underline{J}_s$ since it ordinarily does not affect either the input impedance or far-zone fields"? The answer is two-fold. First, "thin-wire" computer programs are in such widespread use that any information relative to the basic approximations made in these codes is of value. Secondly, there are quantities which the ϕ dependence of $\underline{J}_s$ does affect. For example, the conductor loss resistance is a strong function of the circumferential distribution of current on the wire [1]. A

knowledge as to how this loss resistance varies with wire radius and wire spacing is important in determining the efficiency of such antennas as the electrically small multiturn loop antennas. The ϕ dependence of $\underline{J}_s$ can also be important to the transient behavior [10].

IV. CONCLUSION

This paper has considered the problem of determining the circumferential current distribution on closely spaced electrically thin-wires. The solution is a modification of the piecewise-sinusoidal reaction formulation for thin-wire structures. A Fourier series is used to represent the ϕ dependence of the wire surface current density. Numerical data presented illustrate that there can be a considerable circumferential variation even when the wire to wire separation exceeds several wire diameters. This can be important in determining antenna efficiency; however, if these wires were to be analyzed by "thin-wire" theory (i.e., neglecting the circumferential variation of the surface current density) the correct impedance and far-zone fields are usually obtained.

REFERENCES

[1] G. Smith, "The Proximity Effect in Systems of Parallel Conductors and Electrically Small Multiturn Loop Antennas," Technical Report No. 624, December 1971. Division of Engineering and Applied Physics, Harvard University; prepared under Contract N00014-67-A-0298-0005, NR-371-016 for the Joint Services Electronics Program.

[2] G. O. Olaofe, "Scattering by Two Cylinders," Radio Science, Vol. 5, No. 11, November 1970, pp. 1351-1360.

[3] J. H. Richmond, "Radiation and Scattering by Thin-Wire Structures in the Complex Frequency Domain," Report 2902-10, July 1973. The Ohio State University ElectroScience Laboratory, Department of Electrical Engineering; prepared under Grant No. NGL 36-008-138 for National Aeronautics and Space Administration.

[4] V. H. Rumsey, "Reaction Concept in Electromagnetic Theory," Physical Review, Vol. 94, 15 June 1954, pp. 1483-1491.

[5] S. A. Schelkunoff, "On Diffraction and Radiation of Electromagnetic Waves," Physical Review, Vol. 56, 15 August 1939, pp. 308-316.

[6] R. F. Harrington, Field Computation by Moment Methods, The MacMillan Co., New York, 1968.

[7] W. A. Imbriale and P. G. Ingerson, "On Numerical Convergence of Moment Solutions of Moderately Thick Wire Antennas Using Sinusoidal Basis Functions," IEEE Transaction on Antennas and Propagation, Vol. AP-21, May 1973, pp. 363-366.

[8] J. H. Richmond, "Computer Program for Thin-Wire Structures in a Homogeneous Conducting Medium," Report 2902-12, August 1973, The Ohio State University ElectroScience Laboratory, Department of Electrical Engineering; prepared under Grant No. NGL 36-008-138 for National Aeronautics and Space Administration.

[9] J. H. Richmond, "A Wire-Grid Model for Scattering by Conducting Bodies," IEEE Transactions on Antennas and Propagation, Vol. AP-14, November 1966, pp. 782-786.

[10] T. H. Shumpert and D. J. Galloway, "Finite Length Scatterer Near Perfectly Conducting Ground - A Transmission Line Mode Approximation," IEEE Transactions on Antennas and Propagation, Vol. AP-26, No. 1, January 1978, pp. 145-151.

APPENDIX C

SMALL ANTENNA LOCATION SYNTHESIS USING CHARACTERISTIC MODES*

E. H. Newman

The Ohio State University ElectroScience Laboratory
Department of Electrical Engineering
Columbus, Ohio 43212

11 September 1978

ABSTRACT

It is shown that the efficiency of a small antenna can be substantially increased by properly locating it on its support structure. Characteristic modes are used to determine the optimum location and frequency.

---

*The work reported in this paper was supported in part by Contract N00014-78-C-0049 between Department of the Navy and The Ohio State University Research Foundation.

I. DISCUSSION

An important problem in antenna design is the development of relatively efficient electrically small radiating elements. The antenna efficiency can be defined as

$$E = \frac{R_r}{R_r + R_\ell} \tag{1}$$

where R_r is the radiation resistance and R_ℓ is the loss resistance. Small antennas are generally very inefficient because their radiation resistance is low. The radiation resistance of a small dipole varies as $(\ell/\lambda)^2$, while that of a small loop varies as $(\ell/\lambda)^4$ where ℓ is the maximum extent of the antenna and λ is the wavelength. There are two conventional approaches to improving the efficiency of small antennas. The first is to reduce the loss resistance, say by using thick highly conducting wires to construct the antenna, or by using low loss components in the tuning or matching networks. The second is to increase the radiation resistance, say by top loading a short dipole or ferrite loading a small loop. Below is described a third technique for increasing the radiation resistance.

Small antennas are usually designed on test beds resembling either free space or an infinite ground plane. However, in use they are often mounted on support structure such as a ship, a tank, a man, or an airplane. The basic idea here is to think of the small antenna not as the primary radiator, but rather as a probe to excite currents on the support structure. Since the support structure often is not electrically small it can be an effective radiator. Thus, the radiation resistance and efficiency of a small antenna can be increased by properly locating it on its support structure.

One problem is where to locate the small antenna. Some locations may result in substantial improvements in efficiency, while others may result in little or no improvement. A second and related problem is the selection of an operating frequency which optimizes the efficiency. The optimum location at one frequency may not be the optimum at another frequency. The antenna designer may not have complete freedom in selecting location and frequency. However, knowledge as to how the efficiency varies with frequency and location can help in the selection of the best allowable optimum.

In order to select the optimum location and frequency one could compute and plot a family of curves of efficiency versus position versus frequency. Presented here is a technique which should involve considerably less computation, and also give more physical insight. The technique involves the computation of the characteristic modes of the support structure. The theory of characteristic modes has been presented by Garbacz [1] and by Harrington and Mautz [2]. Numerically efficient techniques, using the method of moments, for computing characteristic modes have also been presented by Harrington and Mautz [3], and are applied in this work.

The characteristic modes are real currents on the surface of a conducting body. Denoting $\underline{J}_n$ as a characteristic mode, the choice $\underline{J}_n$ as a basis set for the current diagonalizes the impedance matrix or operator of the conducting body. The characteristic modes have orthogonality of the radiated fields. Associated with each characteristic mode $\underline{J}_n$ is a real characteristic value or eigenvalue λ_n.

The eigenvalues are important because they tell how well a particular mode radiates. Those modes with small $|\lambda_n|$ are good or effective radiators, while those with large $|\lambda_n|$ are poor or ineffective radiators. In order

to substantially improve the efficiency of a small antenna mounted on a support structure, it is necessary to excite modes which are effective radiators, i.e., those with small $|\lambda_n|$. Associated with each eigenvalue is a characteristic angle defined by

$$\alpha_n = 180^\circ - \tan^{-1}(\lambda_n). \tag{2}$$

Modes with characteristic angles near 180° are effective radiators, while those with characteristic angles near 90° or 270° are ineffective radiators.

A source or probe, with impressed field $\underline{E}^i$, excites the n^{th} characteristic mode with strength

$$V_n = \iint_S \underline{J}_n \cdot \underline{E}^i \, ds \tag{3}$$

where the integral extends over the surface of the body. Equation (3) shows that in order to excite $\underline{J}_n$ as strongly as possible, the probe should be placed at or near the maximum of $\underline{J}_n$. Further, the probe should be oriented so that $\underline{E}^i$ and $\underline{J}_n$ are parallel. Thus, to improve the efficiency of a small antenna we wish to locate it on its support structure where a characteristic mode, with characteristic angle near 180°, is maximum. The design example below will illustrate this procedure for a small loop on a crossed wire.

II. DESIGN EXAMPLE

A design example will now be presented to illustrate the use of characteristic modes to select the operating frequency and location for a small loop on a crossed wire. The crossed wire is shown in the insert in Figure 1, and could represent a crude model for an airplane shape. As a design restriction we will assume that the loop must be located on the longer vertical wire of length L.

The design is begun by computing the characteristic modes and characteristic angles of the crossed wire versus frequency. Figure 1 shows a plot of the characteristic angles of the first few modes versus L/λ. The optimum frequencies are those where the various modes are resonant, i.e., $\alpha = 180^{\circ}$. Figure 2 shows a plot of the characteristic modes at $L/\lambda = 0.75$ where mode C is nearly resonant. In this figure the solid line represents the current on the vertical wire of length L, while the dotted line represents the current on the horizontal wire of length 2L/3. The arrows indicate the direction of current flow. The characteristic angles of the modes are also shown. Note that modes A and D have angles near 90° and 270°, respectively. Thus, they are poor or ineffective radiators and we have no interest in exciting them. Mode B, with $\alpha = 148^{\circ}$, is a reasonably good radiator, but it has zero current on the vertical wire where the small antenna must be located. Thus, we will not be able to excite mode B with substantial strength. Finally, mode C is an excellent radiator with $\alpha = 178^{\circ}$. It has maximum current just above the wire junction, and thus this is the optimum location of the small loop.

Figure 3 shows a plot of the radiation resistance of a small loop, normalized to its value in free space, versus the loop position on the crossed wire at $L/\lambda = 0.75$. The ratio R_r/R_{ro}, where R_{ro} is the radiation resistance of the loop in free space and R_r is the radiation resistance of the loop on the crossed wire, is equal to the increase in efficiency due to the crossed wire, provided the efficiency is low. Note, that as predicted above, the radiation resistance increases substantially (by a factor of about 65) when it is located just above the junction. On the other hand, if a location below the junction ($s<1.0$) is chosen then the increase is less than about a factor of two.

III. SUMMARY

It has been demonstrated that the radiation resistance and efficiency of a small antenna can be substantially increased by properly locating it on its support structure. Characteristic modes are shown to be a useful tool for determining the optimum location and operating frequency. For two reasons, the technique is best applicable to support structures which are not electrically large. First, the size of the moment method impedance matrix, necessary for the computation of the characteristic modes, can become impractically large. Second, as the electrical size of the support structure increases, more and more characteristic modes are effective radiators. In this case, the exact antenna location and operating frequency is likely to be far less critical.

REFERENCES

1. R. J. Garbacz and R. H. Turpin, "A Generalized Expansion for Radiated and Scattered Fields," IEEE Trans. Ant. and Prop., Vol. AP-19, May 1971, pp. 348-358.

2. R. F. Harrington and J. R. Mautz, "Theory of Characteristic Modes for Conducting Bodies," IEEE Trans. Ant. and Prop., Vol. AP-19, September 1971, pp. 622-628.

3. R. F. Harrington and J. R. Mautz, "Computation of Characteristic Modes for Conducting Bodies," IEEE Trans. on Ant. and Prop. Vol. AP-19, September 1971, pp. 629-639.

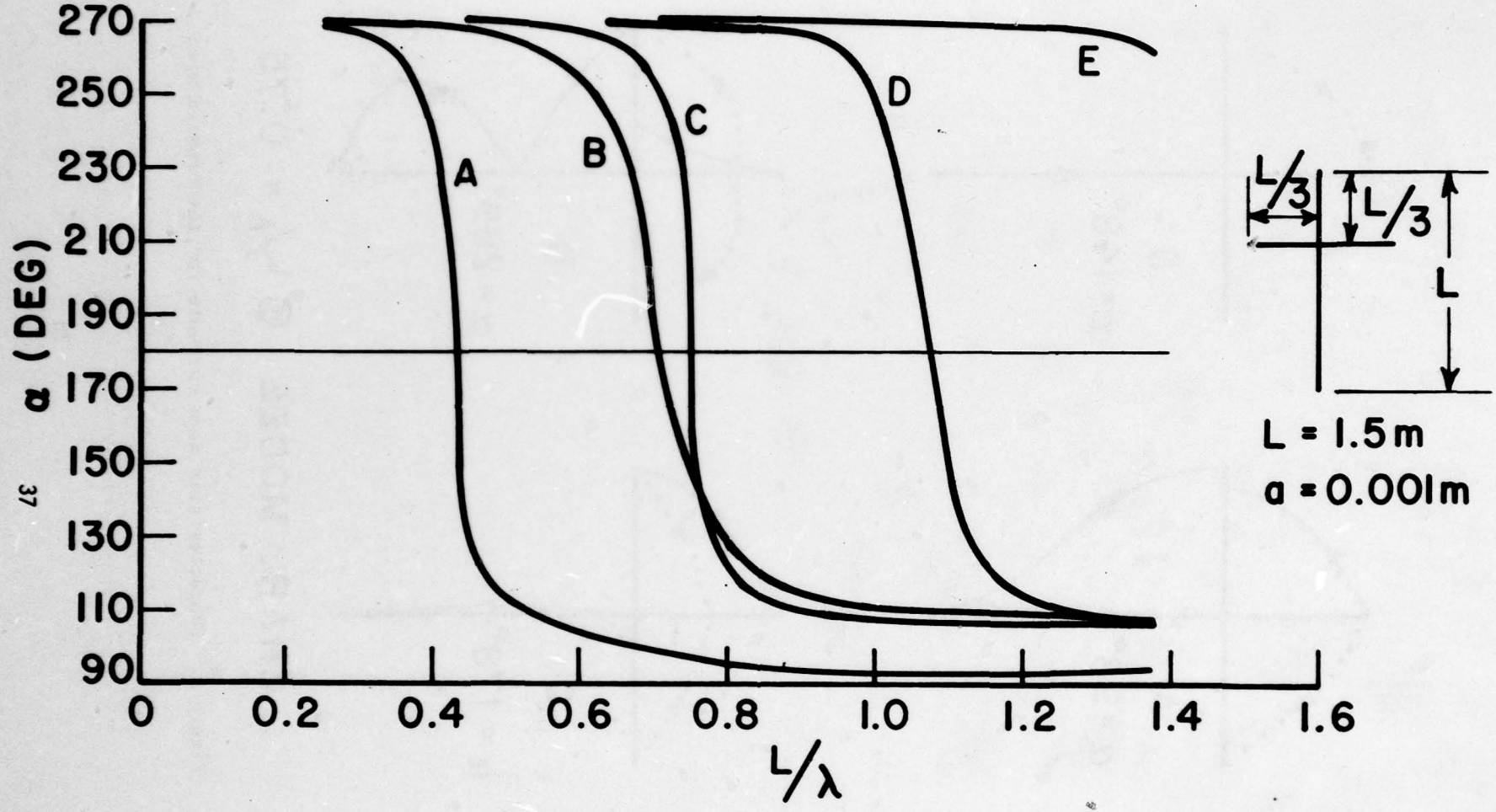

Figure 1. Characteristic angles for the crossed wire.

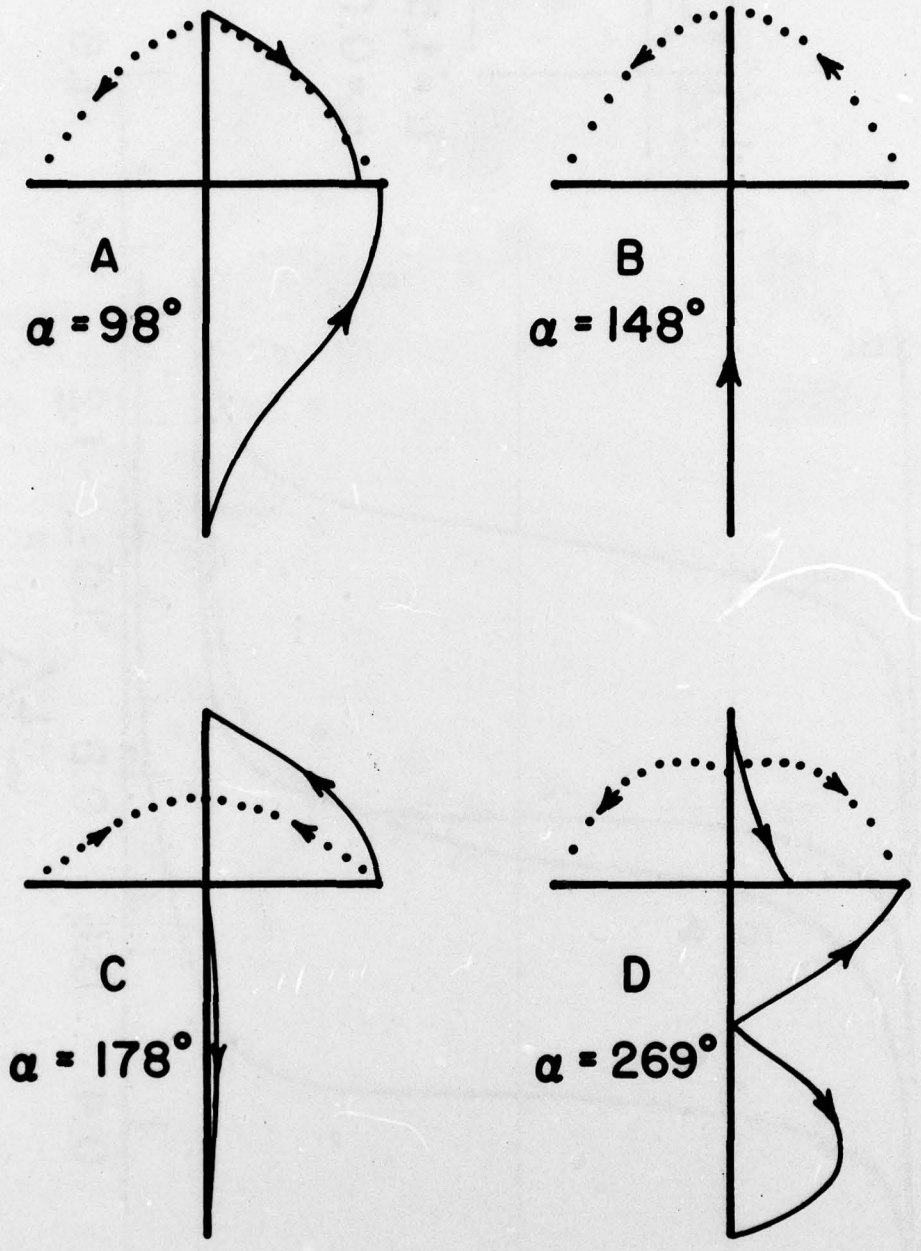

Figure 2. Characteristic mode currents for the crossed wire.

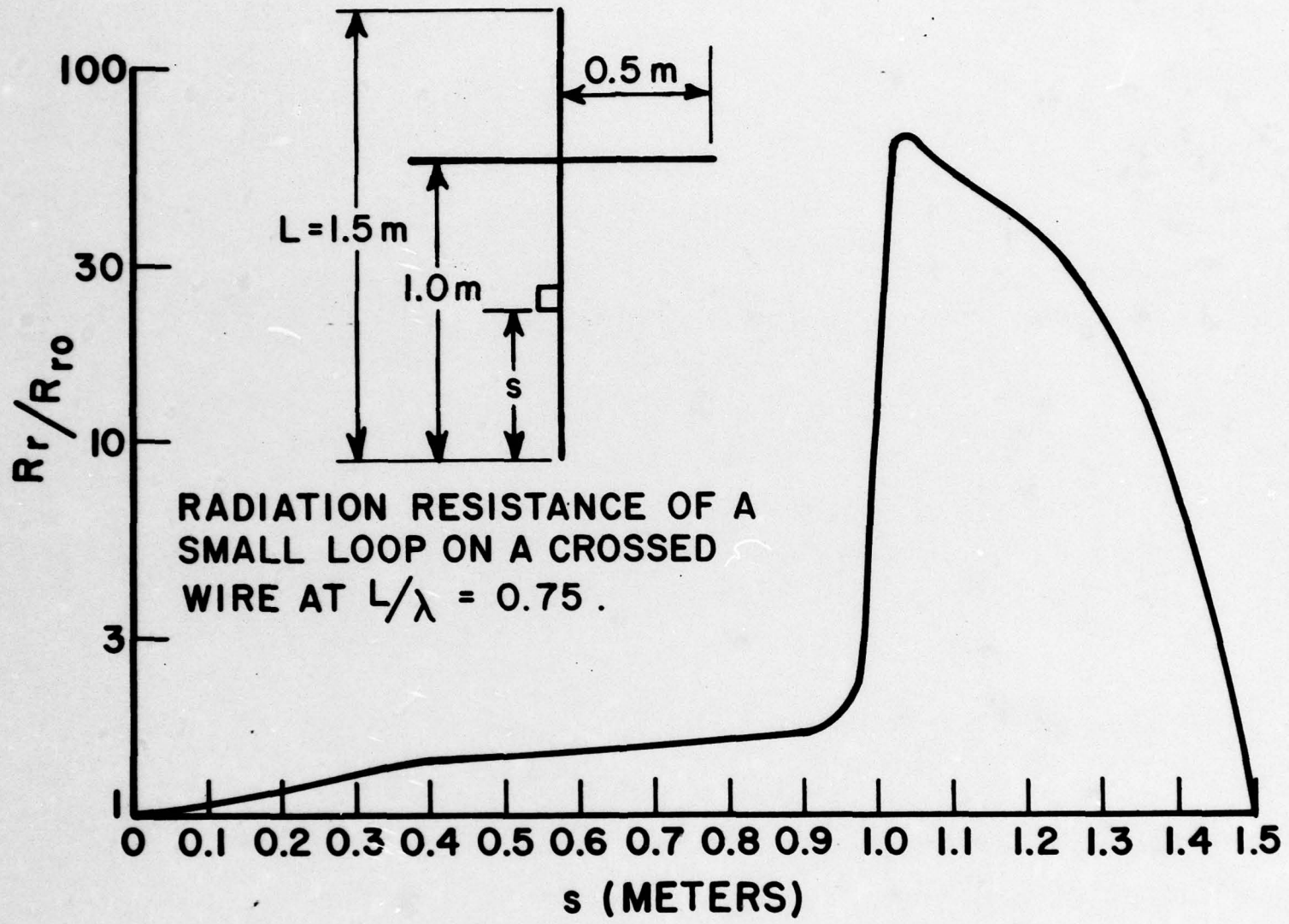

Figure 3. Radiation resistance of a small loop on a crossed wire.